[CANCER RESEARCH 59, 6074–6079, December 15, 1999]

Advances in Brief

Tissue-specific Expression of Functional Isoforms of Mouse Folylpoly-γ-glutamate Synthetase: A Basis for Targeting Folate Antimetabolites[1]

Fiona B. Turner, John L. Andreassi II, Jennifer Ferguson, Steven Titus, Archie Tse, Shirley M. Taylor, and Richard G. Moran[2]

Departments of Pharmacology and Toxicology [F. B. T., J. L. A., R. G. M.] and Microbiology and Immunology [S. M. T.] and the Massey Cancer Center [J. F., S. T., A. T., S. M. T., R. G. M.], Medical College of Virginia, Virginia Commonwealth University, Richmond, Virginia 23298

Abstract

Folates and folate antimetabolites are metabolically trapped in mammalian cells as polyglutamates, a process catalyzed by folylpoly-γ-glutamate synthetase (FPGS). Using 5′-rapid amplification of cDNA ends, RNase protection assays, transfection of cDNAs into FPGS-deficient cells, and kinetic analysis of recombinant enzymes expressed in insect cells, it was determined that the species of active FPGS in mouse liver and kidney was different from that in mouse tumor cells, bone marrow, and intestine. The NH_2-terminal peptide of hepatic enzyme contained 18 amino acids not found in enzyme from dividing tissues, and the specificity of the two isoforms for antifolates also differed, suggesting different architecture of the active sites. In most tissues, the expression of one isozyme or the other was an all-or-nothing event. The exclusive use of one of two alternative sets of initial coding exons in different tissues underlies this phenomenon, suggesting the design of antifolates specific for activation by individual FPGS isoforms and hence tissue-selective targeting of antifolate therapy for cancer, arthritis, or psoriasis.

Introduction

Folate antimetabolites were the first class of agents found to produce complete remissions of human leukemias (1), and the several known classes of antifolates are both potent antiproliferative and cytotoxic therapeutic agents (2–4). The prototypical antifolate, methotrexate, has an established place in the treatment of several human cancers as well as psoriasis and rheumatoid arthritis (2, 5, 6). Antifolates that have a "classical" structure (*i.e.*, those that closely resemble the naturally occurring folates in having a heterocycle linked to *p*-aminobenzoylglutamate, such as methotrexate, lometrexol, and tomudex) rely on transport through the plasma membrane by specific carrier-mediated systems (7–9) followed by metabolism to polyglutamate derivatives by the enzyme FPGS[3] (10, 11). Both of these processes are common to the pathway of intracellular retention used by dietary folates. In human leukemic cells, FPGS is expressed as two forms that differ by the presence or absence of a leader sequence that directs one species to the mitochondria (12). There have been hints that there is a second level of heterogeneity between the species of FPGS expressed in different tissues; for instance, the substrate specificity of crude enzyme from normal mouse intestine was reported to be substantially different from that expressed in several mouse tumors (13). Likewise, slight differences in the kinetics of FPGS between subtypes of human leukemias that are sensitive and resistant to methotrexate have been reported (14). This has led to the speculation that it might be possible to design folate antimetabolites that are only metabolized by enzyme expressed in some tumors, and not by enzyme expressed in the tissues usually at risk with cytotoxic cancer chemotherapy. However, direct evidence that any differences detected in the substrate specificity of FPGS in normal and tumor tissues are due to primary amino acid sequence differences in expressed species of FPGS has remained elusive. We now report that isoforms of functional FPGS that differ in substrate specificity exist in mouse tissues and tumors, that the pattern of expression of these different species of FPGS is not that predicted by previous literature (13, 15), and that the differences in substrate specificity can unambiguously be attributed to differences in the sequences of NH_2-terminal peptides in the different expressed FPGS isoforms.

Materials and Methods

5′-RACE. Poly(A)$^+$ RNA from mouse liver or L1210 cells was reverse transcribed with Superscript II (Life Technologies, Inc.) using an antisense primer (AAGAAGCCGGTCTTCAGGC) in exon 4 of the murine FPGS gene. A polydeoxycytidylate tail was added with terminal deoxynucleotidyl transferase, and PCR was performed using a second, internally nested antisense primer in exon 4 (CGTAATTCCGCAGGATTCGTTCG or, in other preparations, CGTTCGGTGAAGGCACAGG) and a 5′ anchor primer. The resultant PCR products were ligated into pCRII (Invitrogen) and transformed into XL-1 Blue cells. Clones were manually sequenced using Sequenase 2 (United States Biochemical/Amersham).

Transformation of cDNAs for FPGS Species into AUXB1 Cells. The functional activity of FPGS species was tested by transforming cDNA constructs into FPGS-null function AUXB1 cells (16, 17). Exon A1b linked to exons 2–8 or exons 1–8 were generated by reverse transcription-PCR using random-primed mouse liver or L1210 cDNA as a template, respectively. PCR was carried out using an editing mixture of Taq and *Vent* polymerases. Sense primers included each start ATG (bold) and a 5′ *Hin*dIII site (italics): (*a*) mouse liver upstream ATG, 5′-CACG*AAGCTT*CAAGTG**ATGATG**AAAAGCAGGA; (*b*) mouse liver downstream ATG, 5′-GAGT*AAGCTT*GCAGCC**ATG**GAGTGGAAGGACCCATTCCCA; (*c*) L1210 upstream ATG, 5′-CTAT*AAGCTT*AAGACT**ATG**TCGTGGGCGCGGAGCCGAC; and (*d*) L1210 downstream ATG, 5′-CTCT*AAGCTT*CCGGGC**ATG**GAGTATCAGGATGCTGTGC. The antisense primer (5′-ATGCCCCCTTTCTGCCATGC) was located in exon 8, downstream of a unique *Acc*I restriction site. PCR products were cloned into pCRII and verified by sequence analysis. Inserts were released by digestion with *Hin*dIII and *Acc*I and gel-purified. Exons 8 through the polyadenylation signal were isolated as a 1.5-kb *Acc*I-*Eco*RI fragment of murine leukemia cell FPGS cDNA (18) obtained from Dr. David Goldman (Albert Einstein Cancer Center, Bronx, NY). Each 5′-fragment was ligated to this 3′-fragment and *Hin*dIII/*Eco*RI-cut pcDNA3. Clones were verified by restriction enzyme analysis and limited sequencing to verify the 5′ ends and start methionines.

The four cDNA expression plasmids were transfected by calcium phosphate precipitation into AUXB1 cells (5×10^4 cells/100-mm dish). Clones of transfectants were subsequently selected for integration of plasmid in modified α^+ medium [containing 1.2 mg/ml G418, 10 mg/liter thymidine, purines (ribo and deoxyribo adenine and guanine nucleosides, each at 10 mg/liter) and 50 mg/liter glycine] for complementation of cytosolic purine and thymidine

Received 8/23/99; accepted 10/28/99.

The costs of publication of this article were defrayed in part by the payment of page charges. This article must therefore be hereby marked *advertisement* in accordance with 18 U.S.C. Section 1734 solely to indicate this fact.

[1] Supported in part by Grant CA-39687 from the National Institutes of Health, DHHS.

[2] To whom requests for reprints should be addressed, at Massey Cancer Center, Medical College of Virginia, Virginia Commonwealth University, 401 College Street, P. O. Box 980037, Richmond, VA 23298-0230. E-mail: rmoran@hsc.vcu.edu.

[3] The abbreviations used were: FPGS, folylpoly-γ-glutamate synthetase (EC 6.3.2.17); 5′-RACE, 5′-rapid amplification of cDNA ends; DDATHF, 5,10-dideazatetrahydrofolate; poly(A)$^+$ RNA, polyadenylated RNA; nt, nucleotide.

auxotrophy, in $\alpha-$ medium (containing G418 but lacking nucleosides) or for complementation of the mitochondrial glycine auxotrophy (α^+ medium without glycine but with G418). Selection was applied 48 h after transfection. Colonies were fixed and stained with Giemsa 10–12 days after transfection. Three to five plates were used for each condition in each of seven experiments. In some experiments, lower cell numbers (2×10^3 cells/100-mm dish) were transfected, and selection was only for the integration of plasmid with G418. One isolated colony was picked from each dish and mass-cultured, and the phenotype of cells expressing FPGS was tested by plating 120–150 cells/dish and then changing to selective media supplemented with glycine or purine and thymidine.

Preparation and Purification of Recombinant Enzymes in Insect Cells. The coding region of each cDNA clone for mitochondrial and cytosolic FPGS species was cut from the pcDNA3 clones used in Fig. 2*C*, inserted into pFastBac (Life Technologies, Inc.), and used to transform DH10-Bac cells. A recombinant bacmid was selected for each protein, and purified bacmid DNA was introduced into Sf9 insect cells growing as a monolayer using the Cellfectin reagent (Life Technologies, Inc.). Virus produced by these cells was used to infect Sf9 cells at a multiplicity of infection of 1.3. The cells were harvested after 48 h, and enzymes were purified by 30% ammonium sulfate precipitation, followed by sequential Sephacryl S-100/HR (Pharmacia) and DEAE-Sephacel chromatography, a procedure previously used for purification of human CEM cell cytosolic FPGS expressed in insect cells (19). This sequence brought both mouse liver and L1210 cytosolic FPGS species to near electrophoretic homogeneity; these purified enzymes were used in kinetic experiments.

RNase Protection Assays. 5′-RACE products cloned in pCRII were used to generate riboprobes and standard RNAs by *in vitro* transcription. The probe to quantitate RNA species in which A1b sequence (Fig. 2*B*) was linked to exons 2–4 contained the cDNA found in mouse liver from a *Nco*I site at nt 69 in exon A1b to nt 335 in exon 4 [+1 was the A of the mitochondrial translational start codon (12)]. The exon 1/2–4 probe contained the cDNA generated by 5′-RACE using mouse liver mRNA from a *Tth*111I site at nt 34 in exon 1 to nt 364 in exon 4. RNA transcripts were generated from linearized cDNAs using [α-^{32}P]UTP and either the SP6 or T7 RNA polymerase. RNase protection assay reactions contained deionized formamide, 2×10^5 cpm of probe, and 4 μg of poly(A)$^+$ RNA for all tissues except bone marrow, for which 1.5 μg were used. Reactions were hybridized at 50°C overnight, and the samples were incubated with 100 μg/ml RNase A for 30 min (exon A1b/2–4 probe reactions at 37°C and exon 1/2–4 probe reactions at 16°C). The protected fragments were ethanol-precipitated and run on a 6% polyacrylamide urea gel. The sense complement of the probe sequence was transcribed *in vitro* and used as a RNA standard for each probe. This standard allowed the determination of the exact gel mobility of a specific protected RNA fragment representing a single molecular species.

Results

Isolation of cDNAs Encoding Different Species of FPGS in Mouse Liver and Leukemic Cells. FPGS extracted from mouse liver and FPGS extracted from mouse L1210 leukemic cells display apparent differences in substrate preference, as shown in Fig. 1. The substrates chosen for this study, aminopterin (●) and the 6-*R* (□) and 6-*S* diastereomers of DDATHF (△), are generally taken as metabolically inert in mammalian tissues, with polyglutamation being the only known biotransformation. The kinetics of addition of glutamic acid to the dihydrofolate reductase inhibitor aminopterin by FPGS from liver and leukemic cells was very similar, if not identical, but challenge of the FPGS from these tissues with the 6-*R* and 6-*S* diastereomers of DDATHF (20) revealed some distinct differences. The enzyme from liver formed polyglutamate products from 6-*R*-DDATHF at a rate about the same as that seen with aminopterin, albeit characterized by a somewhat lower Michaelis constant. The 6-*S* diastereomer of DDATHF showed a distinct substrate inhibition with mouse liver enzyme but was otherwise as well accepted as 6-*R*-DDATHF. On the other hand, both 6-*R*- and 6-*S*-DDATHF had very different kinetics than aminopterin with FPGS extracted from mouse L1210 leukemic cells, characterized by a distinctly lower maximal velocity. Some time ago, Rumberger *et al.* (13) also reported differences in the substrate specificities for methotrexate analogues of FPGS expressed by mouse small intestine, L1210 cells, and S-180 sarcoma cells. Although there could be several explanations for the results shown in Fig. 1, a difference in the primary sequence of the FPGS expressed in mouse liver and leukemic cells seems to explain the observation. When mRNA from mouse liver and L1210 cells was reverse-transcribed from a primer complementary to the sequence in exon 4 (15) of the mouse FPGS gene and the upstream sequence of FPGS transcripts in these tissues was determined by 5′-RACE, the sequence of the cDNA from liver and L1210 cells was identical from exons 2–4 but differed upstream of the exon 2/exon 1 border (Fig. 2*A*). Roy *et al.* (15) have reported different species of cDNA isolated from libraries from mouse liver and leukemic cells that agree with these differences and have mapped the initial 5′ cDNA sequence from mouse liver to two alternative exons (A1a and A1b) located approximately 10 kb upstream from the exon 1 used in mouse leukemic cells (Fig. 2*B*). Although the sequence downstream of the exon 1/exon 2 border in our RACE experiments was 100% identical between mouse liver and L1210 cells, the sequence upstream of this border showed only the level of homology expected of random matches (Fig. 2*A*). All (10) of the L1210 cell 5′-RACE clones sequenced showed exon 1 spliced to exon 2; of 11 murine liver 5′-RACE clones, 10 contained exon A1b spliced to exon 2, and 1 had exon 1 spliced to exon 2.

Transfection of FPGS Species into AUXB1 Cells. Examination of the mouse leukemic cell FPGS sequence revealed two ATGs located in exactly the same positions (*boxed* in Fig. 2*A*) of this cDNA that we have previously proven to allow use as translational start codons for the production of mitochondrial and cytoplasmic species of FPGS in human CEM leukemic cells (12). In the mouse liver sequence, two sets of potential start codons were also found (Fig. 2*A*), although they were placed quite differently than those in the leukemic sequence. The fit to consensus for translational initiation of sequence

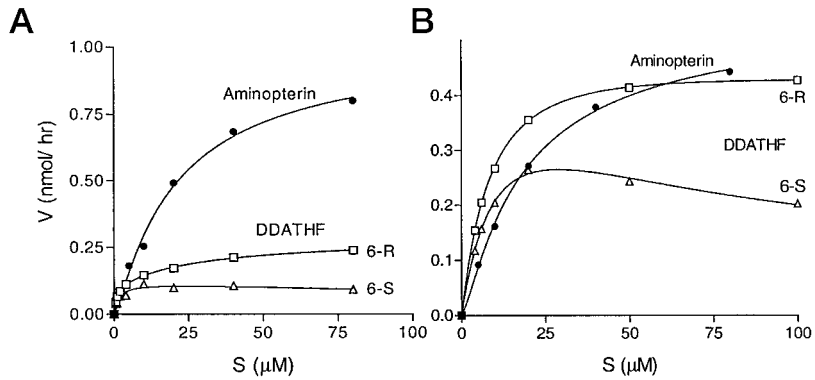

Fig. 1. FPGS extracted from mouse leukemic cells (*A*) has a different preference for folate substrates than FPGS extracted from mouse liver (*B*). Mouse liver was perfused with PBS *in situ* and excised, and mouse L1210 leukemic cells were harvested from the peritoneal cavity of DBA/2 mice. A desalted ammonium sulfate precipitate of a high-speed supernatant fraction was used as a source of FPGS for incubations with the indicated amount of each substrate, and products were isolated by charcoal adsorption (29).

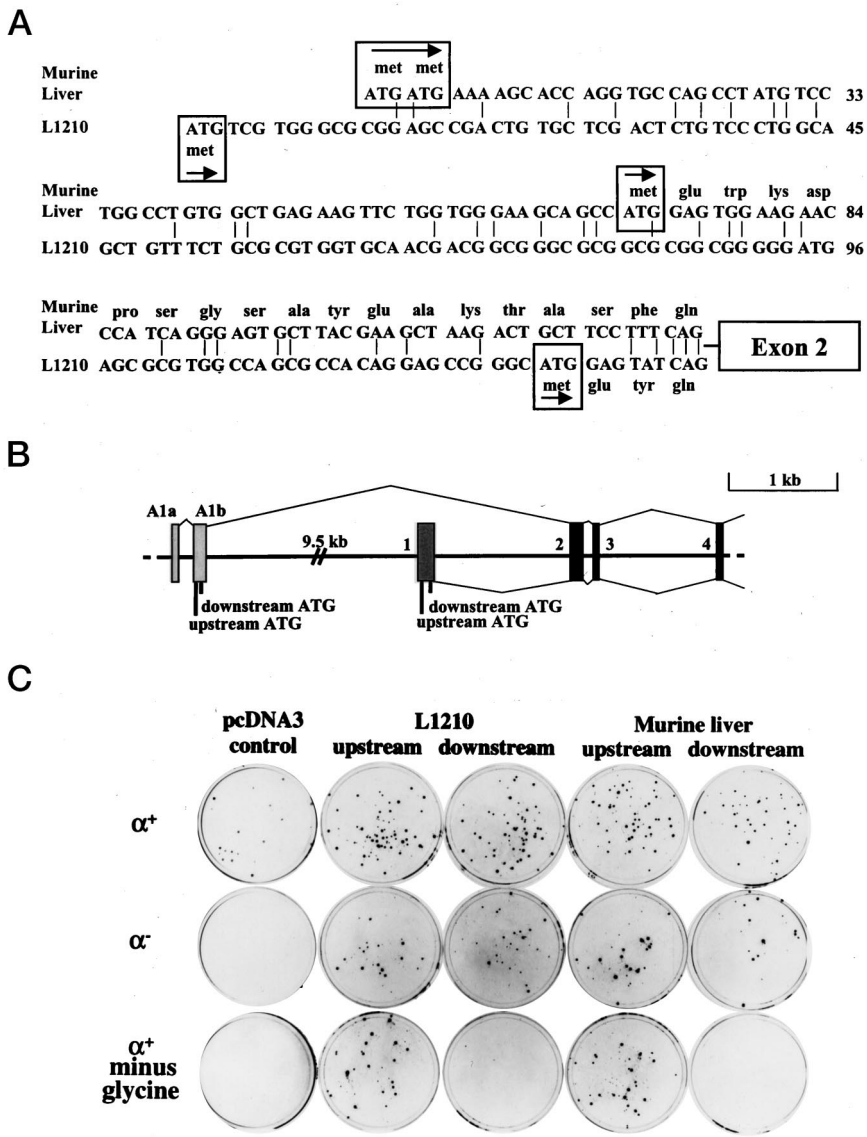

Fig. 2. The FPGS in mouse liver and FPGS in leukemic cells differ in sequence at the NH_2-terminal domain, corresponding to the use of differing initial exons, but both encoded proteins have sufficient FPGS activity to support the growth of mammalian cells. *A*, sequence alignment of cDNA derived from mouse liver and L1210 leukemic cells. 5′-RACE-generated FPGS cDNAs were derived from primers located in exon 4. The sequence of the region of liver and leukemic cell cDNAs corresponding to the cloned segment of exon 4 and exons 2 and 3 were identical, but homology was lost immediately upstream of exon 2. The NH_2-terminal domain of the cytosolic forms of the liver FPGS and the leukemic FPGS differ in sequence over a span of 18 amino acids, as indicated. *B*, a schematic of the murine liver and L1210 splice patterns illustrating the alternative initial exons previously mapped to mouse genomic DNA (15). *C*, complementation of AUXB1 cells by cDNA constructs initiating at putative translational start methionines located in either exon A1b or exon 1. cDNAs cloned into pcDNA3 beginning at each of the *boxed* upstream or downstream ATGs in *A* and containing all downstream exons (2–15) were transfected into AUXB1 cells as calcium phosphate precipitates. Selection of transfectants with G418 began after 48 h in one of three media: (*a*) α^+ media contained G418, thymidine, purines, and glycine and selected only for the integration of pcDNA3; (*b*) α^- media did not contain nucleosides and tested the complementation of the cytosolic purine and thymidine auxotrophy (12); and (*c*) α^+ media without glycine tested the complementation of the mitochondrial glycine auxotrophy.

surrounding the boxed ATG codons in Fig. 2*A* was numerically compared by sequentially multiplying the frequency at which each of the nts at positions −1 to −6 and +4 occurs in the survey performed by Kozak (21). The fit to this consensus of each of the ATGs boxed in Fig. 2*A* was similar to that of the upstream and downstream AUGs in human CEM cell FPGS, both of which are used to initiate translation (13). To directly test the function of these potentially translated open reading frames, cDNAs were constructed corresponding to full-length FPGS sequences initiated at each of the putative start codons noted in Fig. 2. Thus, these cDNA constructs linked exon 1 found in mouse leukemic cells to mouse exons 2–15 and also linked exons A1a and A1b from mouse liver cDNA to exons 2–15. These cDNAs were transfected into AUXB1 cells, a subline of Chinese hamster ovary cells that does not express functional FPGS (17) and, as a result, is auxotrophic for all of the end products of folate metabolism (16). As shown in Fig. 2*C*, all four of these constructs (mouse liver and L1210 sequences from both upstream and downstream putative translational start codons boxed in Fig. 2*A*) allowed synthesis of functional FPGS in AUXB1 cells, complementing either the thymidine and purine auxotrophy of the AUXB1 cells (an indication of restoration of the function of cytosolic FPGS in the transfectants) or the entire phenotype of auxotrophy for thymidine, purine, and glycine. Enzyme assays performed on cell-free extracts of cloned transfectant cell lines confirmed the expression of functional FPGS from all four cDNAs (data not shown). As seen previously with human CEM cells (12), cDNA initiating at the upstream ATG in the L1210 cell sequence complemented the glycine auxotrophy of the AUXB1 cells in addition to the thymidine and purine auxotrophies, indicating that the FPGS species made from the transcript initiating at the upstream ATG was capable of trafficking to and into the mitochondria. The cDNA from leukemic cells using the downstream start methionine complemented only the thymidine and purine auxotrophies, and the transfected cells remained glycine auxotrophs. Likewise, the cDNA constructed from the downstream ATG in the mouse liver sequence complemented only the thymidine and purine synthesis deficiencies typical of cytosolic folate metabolism in the AUXB1 cells, whereas the cDNA initiating at the upstream ATG also complemented the glycine metabolism known to require mitochondrial folate metabolism (12, 22). This pattern was confirmed in experiments in which AUXB1 cells were transfected with the same set of cDNAs, and multiple independent cloned transfectants were selected solely on the basis of expression of G418 resistance; these clones were mass-cultured, and clones that expressed FPGS were phenotyped for requirement of purine and thymidine and/or glycine. The phenotypes of these transfectants were clear:

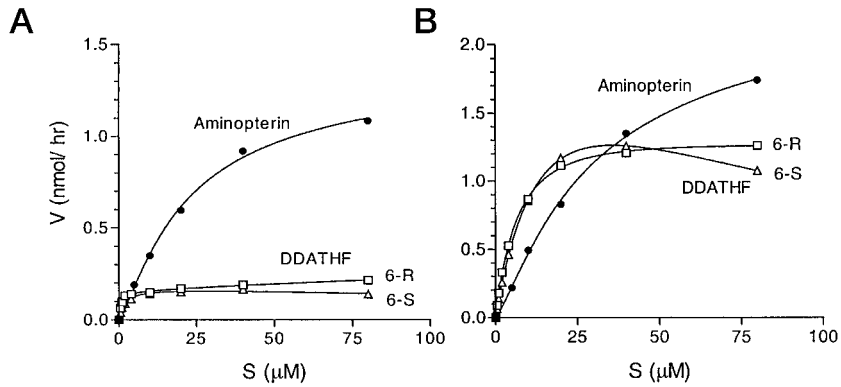

Fig. 3. The kinetics of purified recombinant mouse liver and leukemic cell FPGS. Sf9 cells were infected with recombinant baculoviruses encoding the cytosolic liver and cytosolic leukemic cell forms of mouse FPGS, and the enzyme was extracted from the cells 48 h later. Both enzymes were brought to ≈90–95% purity as described in the text and used for kinetic experiments similar to those shown in Fig. 1. Purified mouse liver FPGS was added to reactions at 0.14 μg/assay and L1210 FPGS was added to reactions at 0.3 μg/assay to give similar product levels, despite the differences in k_{cat} for these enzymes.

cDNA constructs corresponding to FPGS initiating at the upstream ATG in either exon 1 or exon A1b (Fig. 2, *A* and *B*) complemented both cytosolic and mitochondrial folate metabolism; whereas cDNAs initiating translation at the downstream ATGs in either exon 1 or exon A1b complemented only cytosolic folate metabolism (Table 1). The additional 42 amino acids between the two start codons in mouse L1210 cells and the equivalent 23 amino acids in the mouse liver protein both act as mitochondrial leader peptides. Hence, FPGS sequences isolated from mouse liver and those isolated from L1210 cells translate to enzymatically active FPGS *in vivo*, and the tissues direct enzyme to both mitochondrial and cytosolic compartments.

Recombinant L1210 and Mouse Liver Isoforms Are Both Active and Demonstrate the Kinetic Differences Seen with Endogenous Enzymes. Although these results prove that different primary amino acid sequences in the region of the NH_2 terminus of FPGS are compatible with catalytic activity and *in vivo* enzyme function, they do not constitute direct evidence that the differences in substrate specificity seen in Fig. 1 are the result of the sequence heterogeneity shown in Fig. 2*A*. To directly address this question, the cDNAs constructed for the experiments summarized in Fig. 2*C* were recloned into a baculoviral transfer vector, and recombinant viruses were used to express these enzymes in insect cells. These single enzyme species were then purified to near homogeneity, and the experiment of Fig. 1 was repeated on the recombinant FPGS isoforms. With these pure recombinant proteins, the kinetic pattern seen with FPGS extracted from mouse liver and L1210 cells was recapitulated (Fig. 3). Thus, both diastereomers of DDATHF were used by recombinant mouse liver enzyme more efficiently than was aminopterin (Fig. 3*A*), but recombinant L1210 enzyme displayed a distinctly lower k_{cat} when using 6-*R*- and 6-*S*-DDATHF than when using aminopterin (Fig. 3*B*). Data for cytosolic enzyme were used in these experiments, but enzyme produced from recombinant viruses containing the mitochondrial leader sequences of mouse liver and L1210 FPGS showed the same patterns (data not shown). Overall, we drew the conclusions that the differences in the substrate specificity seen in mouse L1210 cells compared to those seen with enzyme from normal mouse liver (Fig. 1) were indeed due to differences in the primary structure of the FPGS made by these tissues and that the NH_2-terminal sequence differences shown in Fig. 2*A* were sufficient to account for the differences seen with endogenous enzyme expressed in mouse liver and leukemic cells (Fig. 1).

Distribution of Isoforms in Mouse Tumor Cells and Normal Tissues. The abundance of these different transcripts and expressed proteins in different tissues cannot be directly assessed from cDNA library screening (23) or 5′-RACE experiments (Fig. 2*A*) due to the potential bias introduced by the reverse transcriptase step in either procedure. Hence, we used RNase protection assays to measure the degree to which this isomorphism is a qualitative or quantitative difference. A very clear but somewhat surprising pattern emerged (Fig. 4): in mouse leukemic cells, only the isoform encoded by the downstream initial exon (exon 1) was present; in mouse liver, the FPGS isoform found was almost exclusively that transcribed from the upstream initial exons (A1a and A1b; Fig. 4*B*). A small amount (approximately 3–5%) of the transcripts for FPGS in mouse liver appeared to include exon 1. The possibility that these minor transcripts were due to blood elements remaining in the perfused livers was ruled out by the observation that FPGS transcripts could not be

Table 1 *Phenotype of AUXB1 cells transfected with cDNAs encoding mouse FPGS species*[a]

Cells	DNA transfected	Colonies formed per plate		
		α^+	α^-	α^+ minus glycine
Controls				
AUXB1	None	181 ± 18	0 ± 0	0 ± 0
CHO	None	192 ± 19	193 ± 5	178
FC2/2D	Human genomic[b]	142 ± 13	134 ± 9	134 ± 22
10-1	pcDNA3	162 ± 16	0 ± 0	0 ± 0
10-2	pcDNA3	226 ± 10	0 ± 0	0 ± 0
cDNA transfectants				
Clone 1-4	L1210 upstream	177 ± 11	172 ± 11	186 ± 5
Clone 1-6	L1210 upstream	172 ± 13	65 ± 6	31 ± 1
Clone 2-2	L1210 downstream	196 ± 7	208 ± 11	0 ± 0
Clone 2-7	L1210 downstream	251 ± 11	254 ± 13	0 ± 0
Clone 3-3	Liver upstream	193 ± 14	188 ± 5	173 ± 5
Clone 3-5	Liver upstream	131 ± 10	140 ± 9	139 ± 8
Clone 4-2	Liver downstream	102 ± 4	111 ± 3	0 ± 0
Clone 4-12	Liver downstream	194 ± 19	189 ± 9	0 ± 0

[a] The indicated cDNAs were transfected into 5000 AUXB1 cells/100-mm dish and selected in α^+ medium supplemented with 1.2 mg/ml G418, and multiple well-isolated colonies were picked and mass-cultured. Cloned transfectants that expressed FPGS were plated at 250 cells/100-mm dish in α^+ medium, and the indicated media were applied after 16 h. Colonies were fixed and stained 10 days later.

[b] See Ref. 12.

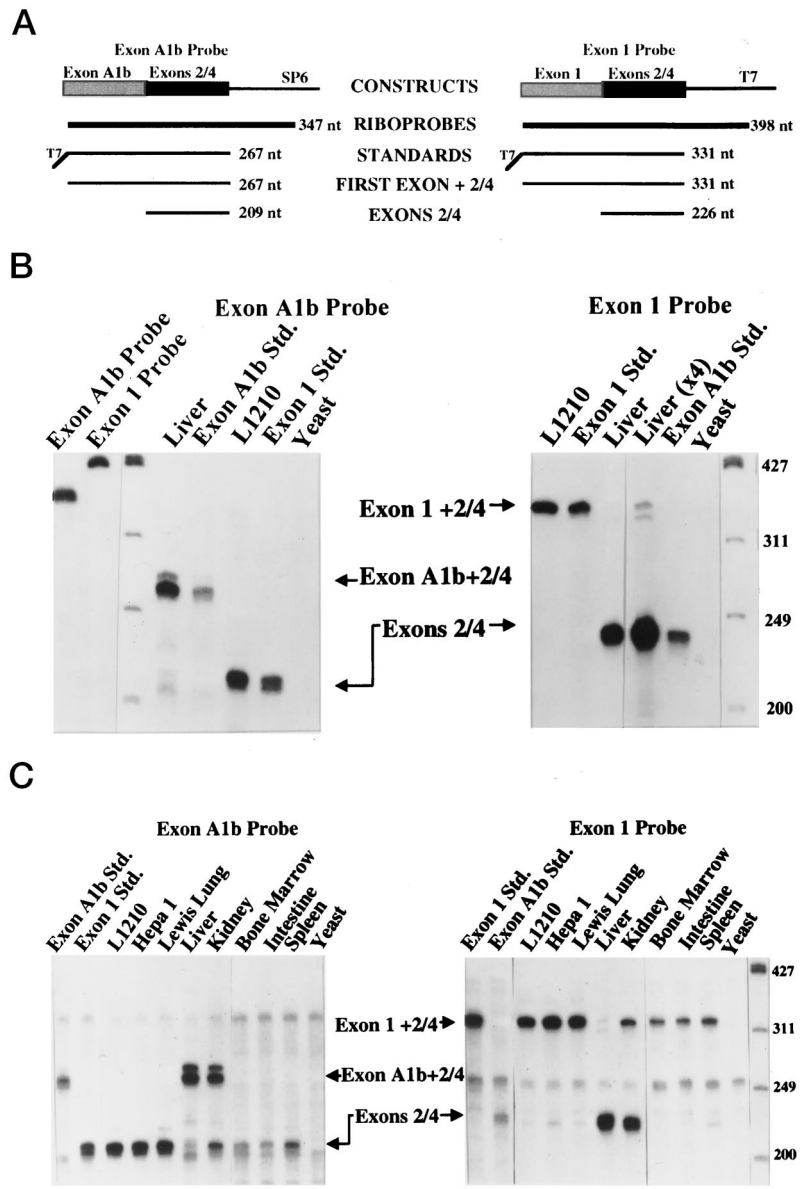

Fig. 4. Tissue specificity of expression of the exon A1b isoform and the exon 1 isoform of mouse FPGS. *A*, schematic diagram of the riboprobes, the PCR-generated RNA standards, and the expected protected fragments in RNase protection assays. *B*, a comparison of isoform expression in murine liver and L1210 cells. The full-length undigested probes are shown on the *far left*. The exon A1b riboprobe, which quantitated the amount of FPGS mRNA in which exons 2–4 are linked to exon A1b (see Fig. 2*B*), was added to the RNA samples in the *left panel*, and the exon 1 probe (corresponding to exon 1 linked to exons 2–4) was added to the RNA samples in the *right panel*. Gels were exposed to film for 14 h, except for the lanes on the *right panel* labeled *Liver (x4)*, *Exon A1b Std.*, and *Yeast*, which were exposed to film for 54 h. ΦX174/*Hin*fI DNA markers are designated in the *far right lane*. *C*, isoform expression patterns in differentiated and dividing tissues and tumors. Riboprobes were generated by *in vitro* transcription with the linearized cDNA templates cloned in pCRII using the SP6 or T7 RNA polymerase binding sites to generate antisense transcripts. The probes were gel-purified and then incubated with 4 μg of poly(A)$^+$ RNA (1.5 μg for bone marrow). A single-stranded RNA standard complementary to the transcribed region of each probe was generated so that the protected product resulting from the standard RNA/probe hybrid would correspond exactly to the RNA segment being examined, as shown in the lanes labeled *Exon 1 Std.* and *Exon A1b Std.* In both panels, lanes for L1210, Hepa1, Lewis lung, liver, and kidney samples were exposed to film for 68 h; the other lanes were exposed to film for 190 h.

detected in mRNA from unfractionated packed blood cells. Examination of the FPGS mRNA expressed in several mouse tumors indicated that the isoform defined in leukemic cells was again exclusively expressed in the HEPA-1 mouse hepatoma and Lewis lung carcinoma (Fig. 4*C*) and also in the Neuro-2a neuroblastoma, S-180 sarcoma, and P19 teratocarcinoma cells (data not shown). Bone marrow and small intestine, the two mouse organs usually limiting to cytotoxic cancer chemotherapy, also expressed the same transcript for the isozyme found in these tumors, as does the spleen, but mouse kidney expressed both the form of enzyme typical of liver and that typical of tumor cells. We conclude that the pattern of differential utilization of the upstream (exons A1a and A1b) and downstream initial exons (exon 1) reflects a mechanism that controls expression of the liver isoform of FPGS in a highly tissue-specific pattern in differentiated cells, but that the form found in leukemic cells is found in many, if not all, dividing cell populations.

Discussion

In this study, we demonstrate that dividing adult mouse tissues, normal or neoplastic, express a different form of FPGS than that found in the few differentiated adult mouse tissues that express FPGS. We do not yet understand why two isoforms of FPGS have evolved, but the precisely controlled use of alternate initial exons of the FPGS gene in differentiated and dividing tissues argues strongly for different functions of the two encoded enzymes.

The definition of isozymes in human tissues is lagging behind the results we show for the mouse. All of the cultured mouse tumor cells we have examined to date express exclusively the FPGS isoform found in normal mouse stem cells. However, a species of FPGS analogous to that we find in mouse liver may be expressed in some human tumors. Should a primary tumor type be found that expresses the FPGS isoform which differs from that in normal human stem cells, it would represent an unprecedented opportunity for rationally designing cancer chemotherapy against that tumor based entirely on differences in the active sites of these FPGS isoforms. This hypothesis remains to be adequately tested.

Using crude preparations of FPGS from mouse tissues, both we (Fig. 1) and Rumberger *et al.* (13) observed differences in the substrate specificity of enzyme expressed in normal mouse tissues and tumors. In our studies, the differences in kinetics seen between FPGS extracted from mouse liver and FPGS extracted from L1210 cells were shown to be

caused by isozyme-specific NH_2-terminal peptides (Fig. 2) by cloning, expressing, and purifying enzymes containing these differences and performing kinetic experiments on these molecularly defined, single enzyme species (Fig. 3). Using crude extracts, Rumberger *et al.* (13) had previously published that crude FPGS from mouse intestine poorly accepted some substrates compared with extracts from L1210 and S-180 cells; aminopterin was used equally well by all of these extracts. Hence, we had originally thought that mouse intestine also expressed a different species of FPGS than mouse tumors, leading to the exciting possibility of selective chemotherapy targeting a tumor isozyme but not the isozyme in drug-limiting intestinal stem cells. This hypothesis was not supported by definitive RNase protection assays, which demonstrated that the same species of FPGS was expressed in mouse tumors, intestine, and bone marrow cells (Fig. 4). This raises the question of why the data of Rumberger *et al.* (13) suggested differences in FPGS based on differences in polyglutamation in experiments with crude enzymes. Two possibilities suggest themselves: (*a*) either the mouse intestinal enzyme differs from the L1210 FPGS due to sequence differences downstream of exon 4; or (*b*) the results from kinetic experiments performed on unpurified enzymes were due to other enzymes in these tissue extracts. For instance, it has been shown that the level of conjugase, which hydrolyzes folylpolyglutamates to their respective monoglutamates, is quite high in the proliferating intestine but is low to undetectable in L1210 cells (24, 25). Hence, kinetic experiments performed on crude extracts (13, 14) might reflect substrate specificity differences of the tissue conjugase rather than FPGS, and any such kinetic differences observed in tissue extracts need to be confirmed by studies on single protein species purified to homogeneity from recombinant systems.

The differences between these two isozymes of FPGS are all at the extreme NH_2 terminus of the protein, in a domain homologous to an α-helix that contacts the critical Ω loop of the *Lactobacillus* casei FPGS (26). The extent to which those structural differences alter the substrate binding site in the mouse liver and dividing cell enzymes is under investigation. As can be seen from Figs. 1 and 3, the k_{cat} for DDATHF is substantially higher for the isozyme expressed in liver than for that expressed in dividing stem cells, although it is clearly not zero in the latter. We would therefore take DDATHF as a lead compound for the development of an antifolate that is a substrate for liver FPGS but not for the enzyme expressed in dividing cells.

An alternative major opportunity for rational drug design is suggested by the specificity of the expression pattern for FPGS isoforms shown herein. Although methotrexate was originally developed for use in cancer chemotherapy (1, 2), it is widely used today for the treatment of rheumatoid arthritis and psoriasis (5, 6). For both of these indications, low doses of methotrexate are given on a chronic schedule. It is commonly the case that hepatic toxicity forces discontinuation of methotrexate therapy, despite the continued activity of the drug. The frequency with which chronic methotrexate initiates severe hepatotoxicity has been estimated to be as high as 23% in recent large-scale trials in psoriatic patients (27). The differences in substrate specificity demonstrated in Figs. 1 and 3 suggest the design of folate antimetabolites that are activated only by the FPGS isoform expressed in actively growing tissues and not by that produced in hepatic tissue. Although the detailed biochemical mechanism of hepatotoxicity of methotrexate is only vaguely understood at the moment, it might be avoided by the selection or design of folate analogues that will not bind to hepatic FPGS. This approach may therefore prevent the onset of the hepatic toxicity seen (27, 28) with long-term low-dose administration of methotrexate in patients with rheumatoid arthritis or psoriasis.

Acknowledgments

We thank Drs. Gordon Ginder and Oliver Bogler for helpful critiques of the manuscript.

References

1. Farber, S., Diamond, L. K., Mercer, R. D., Sylvester, R. F., and Wolf, V. A. Temporary remissions in acute leukemia in children produced by folate antagonist 4-amethopteroylglutamic acid (amethopterin) N. Engl. J. Med., *238:* 787–793, 1948.
2. Bertino, J. R. Ode to methotrexate. J. Clin. Oncol., *11:* 5–14, 1993.
3. Jackman, A. L., Taylor, G. A., Gibson, W., Kimbell, R., Brown, M., Calvert, A. H., Judson, I. R., and Hughes, L. R. ICI D1694, a quinazoline antifolate thymidylate synthase inhibitor that is a potent inhibitor of L1210 tumor cell growth *in vitro* and *in vivo*: a new agent for clinical study. Cancer Res., *51:* 5579–5586, 1991.
4. Smith, S. G., Lehman, N. L., and Moran, R. G. Cytotoxicity of antifolate inhibitors of thymidylate and purine synthesis to WiDr colonic carcinoma cells. Cancer Res., *53:* 5697–5706, 1993.
5. Roenigk, H. H., Auerbach, R., Maibach, H., Weinstein, G., and Lebwohl, M. Methotrexate in psoriasis: consensus conference. J. Am. Acad. Dermatol., *38:* 478–485, 1998.
6. O'Dell, J. Methotrexate use in rheumatoid arthritis. Rheum. Dis. Clin. N. Am., *23:* 779–796, 1997.
7. Goldman, I. D., Lichtenstein, N. S., and Oliverio, V. T. Carrier-mediated transport of the folic acid analogue, methotrexate, in the L1210 leukemia cell. J. Biol. Chem., *243:* 5007–5017, 1968.
8. Jackman, A. L., Gibson, W., Brown, M., Kimbell, R., and Boyle, F. T. *In:* Y. Rustum (ed.), Inhibition of Thymidylate Synthase by Pyrimidines and Folate Analogs: Therapeutic Implications for Cancer Therapy, pp. 274–285. New York: Plenum Press, 1993.
9. Pizzorno, G., Cashmore, A. R., Moroson, B. A., Cross, A. D., Smith, A. K., Marling-Cason, M., Kamen, B. A., and Beardsley, G. P. 5,10-Dideazatetrahydrofolate (DDATHF) transport in CCRF-CEM and MA104 cell lines. J. Biol. Chem., *268:* 1017–1023, 1993.
10. Habeck, L. L., Mendelsohn, L. G., Shih, C., Taylor, E. C., Colman, P. D., Gossett, L. S., Leitner, T. A., Schultz, R. M., Andis, S. L., and Moran, R. G. Substrate specificity of mammalian folylpolyglutamate synthetase for 5,10-dideazatetrahydrofolate analogs. Mol. Pharmacol., *48:* 326–333, 1995.
11. McGuire, J. J., Hsieh, P., Coward, J. K., and Bertino, J. R. Enzymatic synthesis of folylpolyglutamate synthetase: characterization of the reaction and its products. J. Biol. Chem., *255:* 5776–5788, 1980.
12. Freemantle, S. J., Taylor, S. M., Krystal, G., and Moran, R. G. Upstream organization of the multiple transcripts from the human folylpoly-γ-glutamate synthetase gene. J. Biol. Chem., *270:* 9579–9584, 1995.
13. Rumberger, B. G., Barrueco, J. R., and Sirotnak, F. M. Differing specificities for 4-aminofolate analogues of folylpolyglutamyl synthetase from tumors and proliferative intestinal epithelium of the mouse with significance for selective antitumor action. Cancer Res., *50:* 4639–4643, 1990.
14. Longo, G. S., Gorlick, R., Tong, W. P., Ercikan, E., and Bertino, J. R. Disparate affinities of antifolates for folylpolyglutamate synthetase from human leukemia cells. Blood, *90:* 1241–1245, 1997.
15. Roy, K., Mitsugi, K., and Sirotnak, F. M. Additional organizational features of the murine folylpolyglutamate synthetase gene. Two remotely situated exons encoding an alternate 5′ end and proximal open reading frame under the control of a second promoter. J. Biol. Chem., *272:* 5587–5593, 1997.
16. McBurney, M. W., and Whitmore, G. F. Isolation and biochemical characterization of folate deficient mutants of Chinese hamster cells. Cell, *2:* 173–182, 1974.
17. Taylor, R. T., and Hanna, M. L. Folate dependent enzymes in cultured Chinese hamster cells: folylpolyglutamate synthetase and its absence in mutants auxotrophic for glycine + adenosine + thymidine. Arch. Biochem. Biophys., *181:* 331–334, 1977.
18. Spinella, M. J., Brigle, K., and Goldman, I. D. Molecular cloning of murine folylpoly-γ-glutamate synthetase. Biochim. Biophys. Acta, *1305:* 11–14, 1996.
19. Sanghani, P. C., and Moran, R. G. Expression of recombinant human leukemic cell folylpoly-γ-glutamate synthetase in insect cells. Protein Expr. Purif., in press, 2000.
20. Moran, R. G., Baldwin, S. W., Taylor, E. C., and Shih, C. The 6*S*- and 6*R*-diastereomers of 5,10-dideaza-5,6,7,8-tetrahydrofolate are equiactive inhibitors of *de novo* purine synthesis. J. Biol. Chem., *264:* 21047–21051, 1989.
21. Kozak, M. An analysis of 5′-noncoding sequences from 699 vertebrate messenger RNAs. Nucleic Acids Res., *15:* 8125–8148, 1987.
22. Kastanos, E. K., Woldman, Y. Y., and Appling, D. R. Role of mitochondrial and cytoplasmic serine hydroxymethyltransferase isozymes in *de novo* purine synthesis in *Saccharomyces cerevisiae*. Biochemistry, *36:* 14956–14964, 1997.
23. Roy, K., Mitsugi, K., and Sirotnak, F. M. Organization and alternative splicing of the murine folylpolyglutamate synthetase gene: different splice variants in L1210 cells encode mitochondrial or cytosolic forms of the enzyme. J. Biol. Chem., *271:* 23820–23827, 1996.
24. Tse, A., and Moran, R. G. Cellular folates prevent polyglutamation of 5,10-dideazatetrahydrofolate: a novel mechanism of resistance to folate antimetabolites. J. Biol. Chem., *273:* 25944–25952, 1998.
25. Samuels, L. L., Goutas, L. J., Priest, D. G., Piper, J. R., and Sirotnak, F. M. Hydrolytic cleavage of methotrexate γ-polyglutamates by folylpolyglutamyl hydrolase derived from various tumors and normal tissues of the mouse. Cancer Res., *46:* 2230–2235, 1980.
26. Sun, X., Bognar, A., Baker, E. N., and Smith, C. A. Structural homologies with ATP- and folate-binding enzymes in the crystal structure of folylpolyglutamate synthetase. Proc. Natl. Acad. Sci. USA, *95:* 6647–6652, 1998.
27. Malatjalian, D. A., Ross, J. B., Williams, C. N., Colwell, S. J., and Eastwood, B. J. Methotrexate hepatotoxicity in psoriatics: report of 104 patients from Nova Scotia, with analysis of risks from obesity, diabetes, and alcohol consumption during long term follow-up. Can. J. Gasterol., *10:* 369–375, 1996.
28. West, S. G. Methotrexate hepatotoxicity. Rheum. Dis. Clin. N. Am., *23:* 883–915, 1997.
29. Moran, R. G., and Colman, P. D. Measurement of folylpolyglutamate synthetase in mammalian tissues. Anal. Biochem., *140:* 326–342, 1984.

Tissue-specific Expression of Functional Isoforms of Mouse Folylpoly- γ-glutamate Synthetase: A Basis for Targeting Folate Antimetabolites

Fiona B. Turner, John L. Andreassi II, Jennifer Ferguson, et al.

Cancer Res 1999;59:6074-6079.